Superconducting NbN nanowires and coherent quantum phase-slips in dc transport

J. C. Fenton and J. Burnett

***Abstract*—A quantum current standard dual to the Josephson voltage standard has been trumpeted as a primary application for the phenomenon of coherent quantum phase-slips (CQPS) in superconducting nanowires, but it requires a dc transport geometry, distinct from the ring geometry in which CQPS have been probed by microwave spectroscopy measurements. We present measurements on NbN nanowires with width 15 nm and including integrated thin-film resistors to provide a high-impedance environment. Analysis shows that the nanowire behaviour is in line with expectations. The results demonstrate that the process is promising both for future dc transport CQPS measurements and for the fabrication of other circuits in which low-width superconducting nanowires are required.**

This article has been accepted for publication in IEEE Trans. Appl. Supercond. (2016) (http://dx.doi.org/10.1109/TASC.2016.2531005)

***Index Terms*—superconductor–insulator transition, electron-beam lithography, HSQ**

I. Introduction

The discovery of the Josephson effect and consequent Shapiro steps in voltage observed with microwave irradiation enabled the development of the Josephson voltage standard, linked to a fundamental constant rather than an artefact standard, resulting in much more widely realisable primary standards. The quantum nature of the Josephson effect also underlies very high levels of accuracy of the standard, when combined with the ready availability of high-stability frequency sources[1]. Efforts to develop a comparable current standard have continued and the accuracy of state-of-the-art proof-of-principle current standards has now reached better than 1.2 parts in 10^6 [2], still, however, orders of magnitude less good than the accuracy of the Josephson voltage standard, and short of the 1 part in 10^8 required to close the so-called quantum metrological triangle[3] which would provide a consistency check between our understanding of the physical processes underlying the voltage, resistance and current standards.

The authors are with the London Centre for Nanotechnology, University College London, London WC1H 0AH, United Kingdom (email:j.fenton@ucl.ac.uk).

This work was supported by the UK EPSRC under award EP/J017329/1.

The proposal by Mooij and Nazarov [4] that superconducting nanowires could exhibit a physical effect —coherent quantum phase-slips (CQPS)— exactly analogous (dual) to the Josephson effect underlying the Josephson voltage standard has therefore led to considerable interest in the possible realisation of a current-standard device based on the effect. A superconducting nanowire of sufficiently small cross-sectional area can undergo 2π slips in the phase of its order parameter when fluctuations are sufficiently strong. If the nanowire has sufficiently small cross-section and sufficiently high normal-state resistance, quantum fluctuations lead to quantum phase slips. Coherent quantum phase-slips are the exact dual of the Josephson effect, such that a nanowire exhibiting CQPS will pass no current when the applied voltage is below a critical value V_c, exactly dual to a Josephson junction developing no voltage when the applied current is below a critical current. A range of CQPS devices dual to Josephson devices should be possible[5], including, amongst many others, a charge sensor dual to the superconducting quantum interference device (SQUID) and a device dual to the Josephson voltage standard, in which the application of microwaves leads to steps in the passed current separated by $2e\nu$, where ν is the frequency of the microwaves.

Simple considerations lead to the expectation that the rate of independent phase slips in a superconducting nanowire should be much larger in nanowires with small cross-section. One expects an exponential dependence on the superconducting condensation energy of the fluctuating volume ξA, where ξ is the superconducting coherence length and A is the cross-sectional area of the nanowire:

$$\Gamma_\mathrm{S} \sim \exp\left(-\frac{E_\mathrm{cond} A\xi}{k_\mathrm{B}T}\right), \tag{1}$$

where E_cond is the superconducting energy density per unit volume. This rate may be expressed as an energy scale $E_\mathrm{S} = h\Gamma_\mathrm{S}$ or as a corresponding voltage scale $V_\mathrm{S} = 2\pi E_\mathrm{S}/2e$; it may be noted that for thermally activated phase-slips or incoherent quantum phase-slips Γ_S has a physical meaning, but for CQPS E_S is the more physically meaningful parameter, with $V_\mathrm{c} = V_\mathrm{S}$. Theoretical works describing QPS[6] have related its characteristic energy scale E_S to material parameters. While these works differ in details, they share a common exponential dependence, (which corresponds to the exponential dependence in Eq. 1) on $R_\xi = R_\mathrm{N}\xi/l$, where l is the length of the nanowire and R_N is the normal-state

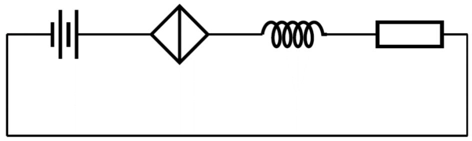

Fig. 1. Basic circuit required for a CQPS current standard. The diamond symbol represents the CQPS element, which we are realising by a superconducting nanowire.

resistance of the nanowire. Mooij *et al.*[7] express $E_{\rm S}$ as

$$E_{\rm S} = a\frac{l}{\xi}k_{\rm B}T_{\rm c}\frac{R_{\rm Q}}{R_\xi}\exp\left(-b\frac{R_{\rm Q}}{R_\xi}\right), \quad (2)$$

where $R_{\rm Q} = h/4e^2 = 6.45\ {\rm k}\Omega$ is the superconducting resistance quantum and a and b are two (positive) constants of order unity which are not expected to be material-dependent. It may be seen that $E_{\rm S}$ is maximised when $R_\xi/R_{\rm Q}$ is as large as possible.

The basic circuit required for realising a CQPS-based current standard is shown in Fig. 1. Its behaviour may be expressed in terms of the (dimensionless) quasicharge q (dual of the phase difference in a Josephson junction), where $I = 2e\cdot{\rm d}q/{\rm d}t$:

$$V(t) = V_{\rm c}\sin 2\pi q + 4\pi eR\frac{{\rm d}q}{{\rm d}t} + 4\pi eL\frac{{\rm d}^2q}{{\rm d}t^2}, \quad (3)$$

where $V(t)$ is the voltage drop across the circuit components, typically set by a voltage bias applied to the circuit and $V_{\rm c}$ is the critical voltage of the CQPS-nanowire element. The series resistance R and series inductance L provide a high-impedance environment for the nanowire and can be chosen to ensure that the quasicharge dynamics entails stable steps rather than chaotic behaviour. Experimentally, the kinetic inductance of a superconducting nanowire makes (wider) sections of nanowire appropriate as inductive elements, and fabricating thin-film resistive elements of a desired value is also relatively straightforward[8]; the focus of attention in a fabrication process is the superconducting nanowire.

Experimental studies of superconducting nanowires have been reported since well before the proposals for a nanowire-based current standard, with observations of resistance below the superconducting $T_{\rm c}$ in superconducting nanowires first being attributed to quantum fluctuations in the 1980s[9]. Since the 1990s, numerous $R(T)$ measurements on superconducting nanowires have been reported in which resistive "tails" persisting below $T_{\rm c}$ have been attributed to QPS and often fitted quantitatively to models including QPS, although in some cases spurious results may have been obtained if careful filtering of measurement lines was not employed. In general, care should be taken not to conclude too readily from $R(T)$ measurements of nanowires alone, even when accompanied by good quantitative fits to QPS models, that a nanowire is undergoing strong QPS, since quantitative fits generally have several adjustable parameters which means a good fit can be found to many data sets with qualitatively the expected behaviour and, moreover, there are other causes such as materials inhomogeneity which could be responsible for resistance below $T_{\rm c}$. To differentiate from such alternative explanations, more evidence such as current–voltage measurements[10] or microwave-irradiation measurements is needed.

Detailed studies in MoGe nanowires[11], [12] revealed a range of behaviour in nanowires of similar dimensions, with some remaining superconducting at low temperature in contrast with predictions that nanowires with normal-state resistance above $R_{\rm Q}$ would undergo a transition to insulating behaviour at low temperature. Recent analysis [7] explains that the insulating behaviour is obtained when the ratio of QPS and inductive energy scales $\alpha \equiv E_{\rm S}/E_L$, where $E_L = \Phi_0^2/2L$ and $\Phi_0 = h/2e$ is the flux quantum, exceeds a certain value, $\alpha_{\rm c}$. Since $\alpha \propto l^2$, in this respect longer wires are desirable for QPS devices. The satisfactory explanation of the data of Ref. [12] implies that high-resistance behaviour in those nanowires was indeed caused by QPS.

Microwave spectroscopy with a superconducting nanowire embedded in a ring geometry has demonstrated CQPS unambiguously[13], [14] and some promising results in the dc transport geometry have also been reported[15], [16], [17] but, to date, a prototype current-standard based on CQPS has not yet been reported. A major factor in this can be identified as the significant technical challenge of realising superconducting nanowires with the properties required for CQPS to result. This challenge arises from the dual requirement of small cross-sectional dimensions and high normal-state resistance[18]. Given that large $R_{\rm N}$ is generally best obtained in two-component superconductors, this latter requirement implies very careful control of material composition, while the requirement of small cross-section itself implies constraints on the maximum acceptable level of non-uniformity in the material.

In this article, we report advanced multi-stage fabrication of a circuit suitable for dc transport measurements of the type required for a quantum current standard. The devices are based on nanowires with typical width 15 nm, approaching the smallest width previously reported for freestanding nanowires[19]. The nanowires are fabricated in NbN, chosen because it allows tuning of composition to achieve high $R_{\rm N}$ while maintaining a superconducting $T_{\rm c}$ practical for characterisation and operation. We report characterisation measurements of the device at temperatures down to 350 mK and analyse the obtained data, concluding that the behaviour of the device is promising for future quantum current-standard device realisations.

II. Fabrication

Nanowires are fabricated from films of niobium nitride, deposited by reactive dc magnetron sputtering on sapphire substrates. For the sample described here, a recipe already identified as leading to films with high uniformity was selected: a 1.8-minute deposition with a 1:1 flow of Ar and N_2 and total pressure of 3.5×10^{-3} mbar was used, along with a sputter power of 200 W, leading to a nominal film thickness of 18 nm. The nanowires are defined by electron-beam lithography (EBL) of 35-nm-thick hydrogen silsesquioxane (HSQ) positive resist, followed by reactive ion-etching for 110 s at 100 W and 100 mTorr with CHF_3 and SF_6 flows of 35 sccm and 14 sccm respectively. Prior to the NbN deposition, CrO_x thin-film resistors[8] are defined by a separate EBL patterning stage using polymethyl methacrylate (PMMA) resist, followed by a 2-minute dc magnetron sputtering stage in an argon atmosphere containing 8% oxygen, followed by liftoff, in a process described in more detail elsewhere[8]. A final nominally-55-nm-thick Au/Cr wiring layer, sputtered onto an EBL-patterned PMMA layer following an *in situ* Ar-ion mill step to remove surface oxide from interfaces, and followed by liftoff, provides electrical contact to the NbN and CrO_x components. Since the sapphire substrate is electrically insulating, a 10-nm gold layer is deposited on top of the resist prior to each EBL stage in order to avoid pattern distortion due to charging. This gold layer is removed by a KI/I_2/H_2O wet-etch dip immediately prior to each development stage. A short oxygen plasma ash step is also included immediately prior to each deposition stage, to promote adhesion. The HSQ resist thickness was chosen carefully with reference to the film thickness and width of the nanowire: too large a resist thickness leads to an overly large aspect-ratio in the defined resist mask and makes the resist nanowire likely to collapse over onto its side. On the other hand, because the selectivity of the etch between NbN and HSQ is limited, too small a thickness of the resist limits the depth of NbN which can be removed before the resist mask is entirely etched away. The etch time is chosen to intentionally etch through the resist mask and remove the top section of the NbN nanowire since it is undesirable for there to be HSQ remaining on top of the final nanowire[20]. This means that the thickness of the final nanowire is less than the thickness of the NbN film originally deposited.

The design used for EBL patterning is shown in Fig. 2. The narrow section in the centre of the NbN nanowire is a single pixel wide in the design and 6 μm long, and is exposed close to optimal exposure dose at 10 kV acceleration voltage, 1280 pC/cm (1150 pC/cm for the wire shown in the insets of Fig.2). It is connected at each end to a wider section of NbN nanowire, which provides additional kinetic inductance, defined by a single-pixel line (over)dosed at 3840 pC/cm (3200 pC/cm for the nanowire shown in Fig. 2). Four connections are made to the nanowire shown in Fig. 2 via CrO_x resistors, two towards each end, such that all measurement leads are connected to the sample only via one of these resistors. As well as ensuring a high-impedance environment for the nanowire, empirically we have found that this configuration makes nanowires more robust. Presumably this is because, during electrostatic discharge events, it is high currents flowing through the nanowire which can destroy it, and the large resistance limits the magnitude of currents flowing during electrostatic discharge events.

Scanning electron microscope (SEM) images of a completed sample are shown in the insets of Fig. 2. The narrow section of nanowire has sections 12 nm wide, with typical widths of this nanowire and other similar nanowires on the same chip being

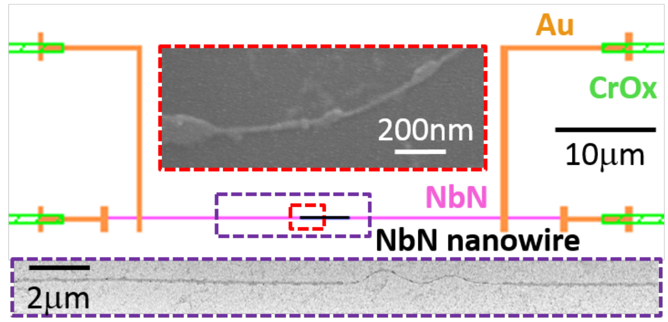

Fig. 2. Design used for the sample reported here, with a 6-μm-long narrow NbN nanowire (black) in the centre broadening at each end to wider NbN inductors (magenta) contacted vertically close to their ends and horizontally at each end by gold wiring (gold!) which is in turn connected to $\sim$100-μm-long CrO_x resistors (green; only part of these is shown). The insets are SEM images of a completed device, with the upper (lower) inset corresponding to the regions indicated schematically in the main panel by the red (purple) dashed rectangle. The lower inset shows an SEM image of the NbN nanowire (the usual contrast is inverted for clarity). The upper inset is a more detailed scan showing the change in nanowire width from the wider to the narrower section, shown with the usual contrast. The homogeneous grainy texture visible in each image is the semi-transparent gold conducting layer deposited on the surface after the device is completed, in order to enable imaging without charging.

15–20 nm. The wider (inductive) section of nanowire has a width of 110 nm. It is immediately noticeable from the image that the narrow section of nanowire has a wavy appearance, in contrast to the straight line in the design. This has arisen because the narrowest sections of the resist mask detached from the substrate during development before re-attaching as a wavy nanowire upon drying. The wavy trajectory is then transferred into the NbN upon etching. As we show below, surprisingly the nanowire remained intact despite detaching and electrical connectivity was maintained in the resulting NbN nanowires. Indeed other nanowires on the same chip showing the same wavy appearance also showed electrical connectivity. It appears that some compressive strain in the resist nanowire during exposure is relaxing once the surrounding material develops away leaving the less rigid narrow nanowire. Similar behaviour has previously been reported and attributed to swelling strain in optimally dosed HSQ resist.[21] Although the still-continuous wavy nanowires are no less functional than a straight wire would be, this behaviour is undesirable because it reduces the yield of devices on any given chip and further investigations are planned to try to eliminate it from future devices.

III. Results and discussion

We conducted electrical characterisation on the chip in a ^{3}He measurement system equipped with copper powder filters and shielded measurement lines. $I(V)$ measurements were made continuously during slow changes in sample temperature down to 350 mK. Fig. 3 shows the low-bias resistance $R(T)$ and Fig. 4 shows $I(V)$ characteristics at selected temperatures.

A superconducting transition is observed centred on 3.7 K, with a relatively broad 10%–90% width of 1.8 K. The T_c is lower than the bulk T_c of NbN (8.5 K for films of this

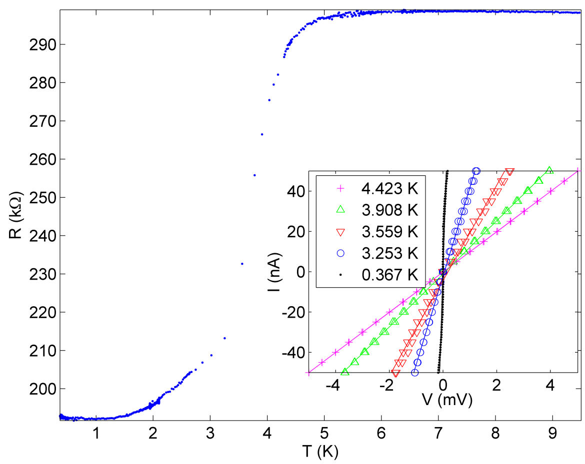

Fig. 3. (Main panel) $R(T)$ for the nanowire, extracted from linear fits to $I(V)$ data collected between ± 50 nA, such as those shown in the inset, measured in a two-probe configuration because this sample had only two leads, so the CrO_x resistors (total length 197.5 μm and width 1 μm and inductive nanowire section (total length 47 μm and width 110 nm) are also measured. Nonetheless, the change in measured resistance with temperature can be attributed entirely to the NbN nanowire (wider and narrower sections in series) since the interface contact resistance is negligible and independent measurements show that the resistance of the CrO_x resistors does not vary significantly over the temperature range shown — as also indicated by the constancy of the resistance above T_c. (Inset) $I(V)$ for the nanowire at selected temperatures. In this plot, in order to show the extent of the linearity more clearly, a resistance of 190.4 kΩ has been subtracted and linear fits added; a small voltage offset has also been subtracted.

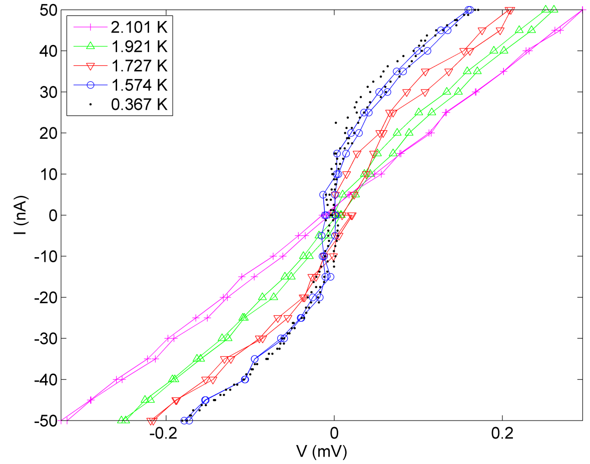

Fig. 4. $I(V)$ for the nanowire at selected temperatures after a resistance of 190.4 kΩ has been subtracted; a small voltage offset has also been subtracted. Lines have been added to show the sequence in which data points were collected.

composition); prior measurements[22] on NbN samples of similar thickness and a range of widths have shown that the T_c of NbN tracks becomes suppressed for tracks with widths below $\sim$100 nm. The inset of Fig. 3 shows that the measured $I(V)$ remains close to linearity down to the lowest measurement temperature. However, careful inspection reveals a small departure from linearity below 2.0 K. This is much more apparent once the CrO_x resistance is subtracted, as shown for selected temperatures below T_c in Fig. 4. At the lowest temperature, the resistance at 50 nA is $\sim$2 kΩ larger than the resistance at 10 nA. The form of this $I(V)$ is at least qualitatively similar to those fitted to incoherent QPS models by Altomare *et al.* although we do not attempt quantitative fitting in the absence of measurements in a 4-point configuration. We are hesitant to conclude that this represents evidence of incoherent QPS below 2 K; we cannot rule out that the features arise from inhomogeneities in the nanowire or nonlinearity in the series components in this two-probe measurement and further investigations are required. We emphasise that explanations related to photons conducted down to the sample along the measurement lines are, however, excluded because of the careful filtering we have employed on the measurement lines.

Given the small cross-section of the nanowires, the relatively long length of the nanowires and the use of a material which exhibits high normal-state resistance, the absence of a more clear upturn in low-temperature resistance associated with strong QPS is at first sight surprising. However, let us take a closer look, following Ref. [7]. Based on the observed physical dimensions of our NbN structure and the measured value of R_N, assuming $\xi = 5$ nm and, using a=0.209 and b=0.115, the values for the material-independent parameters employed in Ref. [7] to successfully model the earlier data[12], we can calculate E_S=1.04$\times 10^{-25}$ J ($V_S \approx 2$ μV). The additional inductive section of NbN nanowire increases the inductance by around 60%, leading to a total inductance of the narrow and wider NbN sections L=250 nH and E_L=8.4$\times 10^{-24}$ J, so $\alpha \sim$0.01, significantly below α_c=0.3 taken in Ref. [7] for the values we have assumed here for a and b and consistent with our observation of superconducting behaviour in the nanowires. Compared to our nanowires, the nanowires analysed in Ref. [7] have smaller values of l/ξ, but generally larger values of R_ξ/R_Q and in fact the $R_\Box$ values for the particular composition chosen for our nanowires here is not particularly high. Indeed for other compositions of NbN we find $R_\Box$ as high as $\sim$ 20 kΩ. By modifying the composition of the nanowire to increase the sheet resistance to around this value, we would expect to move into the realm in which strong QPS is obtained, appropriate for CQPS devices.

IV. Conclusion

We have demonstrated a successful multistage fabrication process for superconducting-nanowire devices in a high-impedance environment. The fabrication process allows us to obtain wires with width below 15 nm. The zero-conductance state associated with coherent quantum phase-slips is not observed in this particular device, but analysis suggests that this lack of evidence for CQPS is in line with expectations given the particular NbN composition used in this sample. Nonlinearity in the low-temperature $I(V)$ *may* be the result of dissipation in the superconducting state due to incoherent QPS. The results are highly promising for future CQPS dc transport measurements on more resistive samples and so for the development of a CQPS quantum current standard, as well as being of technological relevance for the embedding of very narrow superconducting nanowires into circuits for other applications.

REFERENCES

[1] M. Milton, J. Williams, and S. Bennett, "Modernizing the SI: towards an improved, accessible and enduring system," *Metrologia*, vol. 44, pp. 356–364, 2007.

[2] S. Giblin, M. Kataoka, J. Fletcher, P. See, T. Janssen, J. Griffiths, G. Jones, I. Farrer, and D. Ritchie, "Towards a quantum representation of the ampere using single electron pumps," *Nature Communications*, vol. 3, p. 930, 2012.

[3] M. Milton, J. Williams, and A. Forbes, "The quantum metrology triangle and the redefinition of the SI ampere and kilogram; analysis of a reduced set of observational equations," *Metrologia*, vol. 47, pp. 279–286, 2010.

[4] J. Mooij and Y. Nazarov, "Superconducting nanowires as quantum phase-slip junctions," *Nature Physics*, vol. 2, pp. 169–172, 2006.

[5] A. Hriscu and Y. Nazarov, "Coulomb blockade due to quantum phase slips illustrated with devices," *Physical Review B*, vol. 83, Art.ID. 174511, 2011.

[6] K. Arutyunov, D. Golubev, and A. Zaikin, "Superconductivity in one dimension," *Physics Reports*, vol. 464, pp. 1–70, 2008.

[7] J. Mooij, G. Schön, A. Shnirman, T. Fuse, C. Harmans, H. Rotzinger, and A. Verbruggen, "Superconductor-insulator transition in nanowires and nanowire arrays," *New Journal of Physics*, vol. 17, Art.ID. 033006, 2015.

[8] C. Nash, J. Fenton, N. Constantino, and P. Warburton, "Compact chromium oxide thin film resistors for use in nanoscale quantum circuits," *Journal of Applied Physics*, vol. 116, no. 22, Art.ID. 224501, 2014.

[9] N. Giordano, "Evidence for macroscopic quantum tunneling in one-dimensional superconductors," *Physical Review Letters*, vol. 61, pp. 2137–2140, 1988.

[10] F. Altomare, A. Chang, M. Melloch, Y. Hong, and C. Tu, "Evidence for macroscopic quantum tunneling of phase slips in long one-dimensional superconducting Al wires," *Physical Review Letters*, vol. 97, Art.ID. 017001, 2006.

[11] C. Lau, N. Markovic, M. Bocrath, A. Bezryadin, and M. Tinkham, "Determination of the superconductor-insulator phase diagram for one-dimensional wires," *Physical Review Letters*, vol. 87, Art.ID. 217003, 2001.

[12] A. Bollinger, R. Dinsmore, A. Rogachev, and A. Bezryadin, "Determination of the superconductor-insulator phase diagram for one-dimensional wires," *Physical Review Letters*, vol. 101, Art.ID. 227003, 2008.

[13] O. Astafiev, L. Ioffe, S. Kafanov, Y. A. Pashkin, K. Y. Arutyunov, D. Shahar, O. Cohen, and J. Tsai, "Coherent quantum phase slip," *Nature*, vol. 484, no. 7394, pp. 355–358, 2012.

[14] J. Peltonen, O. Astafiev, Y. P. Korneeva, B. Voronov, A. Korneev, I. Charaev, A. Semenov, G. Golt'sman, L. Ioffe, T. Klapwijk, *et al.*, "Coherent flux tunneling through NbN nanowires," *Physical Review B*, vol. 88, no. 22, Art.ID. 220506, 2013.

[15] T. Hongisto and A. Zorin, "Single-charge transistor based on the charge-phase duality of a superconducting nanowire circuit," *Physical Review Letters*, vol. 108, Art.ID. 097001, 2012.

[16] C. Webster, J. Fenton, T. Hongisto, S. Giblin, A. Zorin, and P. Warburton, "NbSi nanowire quantum phase-slip circuits: dc supercurrent blockade, microwave measurements, and thermal analysis," *Physical Review B*, vol. 87, no. 14, Art.ID. 144510, 2013.

[17] J. Lehtinen, T. Rantala, and K. Arutyunov, "Insulating State of a Quasi-1-Dimensional Superconductor," arXiv:1311.3202, 2013.

[18] J. Fenton, C. Webster, and P. Warburton, "Materials for superconducting nanowires for quantum phase-slip devices," *Journal of Physics: Conference Series*, vol. 286, Art.ID. 012024, 2011.

[19] H. Kim, S. Jamali and A. Rogachev, "Superconductor-Insulator Transition in Long MoGe Nanowires," *Physical Review Letters*, vol. 109, p. 027002, 2012.

[20] R. Barends, H. Hortensius, T. Zijlstra, J. Baselmans, S. Yates, J. Gao, and T. Klapwijk, "Contribution of dielectrics to frequency and noise of NbTiN superconducting resonators," *Applied Physics Letters*, vol. 92, Art.ID. 223502, 2008.

[21] S. Regonda, M. Aryal, and W. Hu, "Stability of HSQ nanolines defined by e-beam lithography for Si nanowire field effect transistors," *Journal of Vacuum Science and Technology B*, vol. 26, pp. 2247–2251, 26.

[22] N. Constantino, M. Urdampilleta, C. Nash, J. Burnett, J. Morton, J. Fenton, and P. Warburton in preparation, 2016.